Reverberation mapping the torus in 12 Active Galactic Nuclei using Spitzer and optical light curves

Andrew Robinson[1], Billy Vazquez[1], Michael Richmond[1], Brad Peterson[2], Keith Horne[3], & the Spitzer Torus Reverberation Collaboration

[1]Rochester Institute of Technology, [2]Ohio State University, [3]St Andrew's University

A 2.5-year Spitzer monitoring campaign

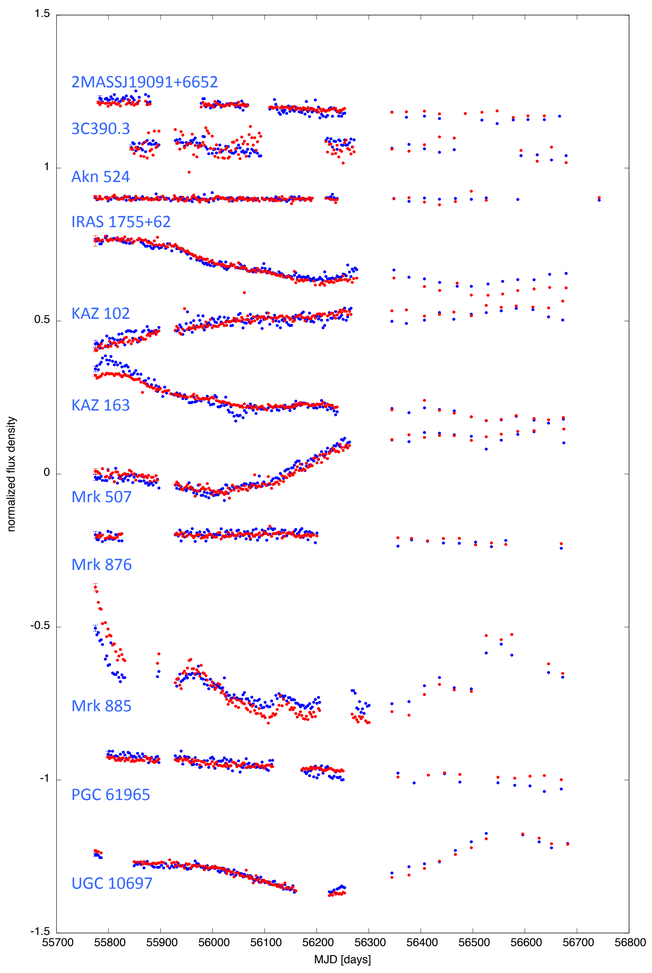

Fig. 1. Light curves at 3.6 μm (blue) and 4.5 μm (red) for 11 AGN (see Fig. 2 for NGC6418). Representative error bars are plotted for the first point in each case..

We present preliminary results from a ~2.5 year Spitzer "Warm Phase" monitoring campaign on 12 broad-line AGN, with the goal of determining the size of the torus at 3.6 and 4.5 μm by "reverberation mapping". The Spitzer observations were obtained during Cycle 8 (Aug 2011 – Jan 2013) at ≈3-day intervals and Cycle 9 (Feb. 2013 – Jan 2014) at 30-day intervals. Supporting optical B and V band observations were obtained with the Liverpool Telescope and the Faulkes Telescope North. We are also using Catalina Sky Survey data to supplement our optical observations. This panel presents some results from the time series analysis of the IR light curves for the entire sample. Below we present the optical–IR reverberation analysis for the most variable object, NGC 6418.

Source	Seyfert Type	$L_{3.6\mu m}$ 10^{42} erg s^{-1}	3.6 μm ΔF/<F>	4.5 μm ΔF/<F>	$\tau_{4.5-3.6}$ days
2MASSJ19091+6652	NLS1	147	0.11	0.06	21.3 (+6.7/-0.3)
NGC6418	S1	4.68	1.02	1.34	11.5 (+1.4/-1.2)
3C390.3	S1	51.0	0.07	0.11	–0.4 (+3.5/-7.1)
AKN524	S1	0.90	0.03	0.08	28.0 (+0.5/-68)
IRAS 17552+6209	S1.9	9.68	0.16	0.17	1.24 (+0.25/-0.27)
KAZ102	S1.2	65.8	0.13	0.15	29.3 (+2.0/-3.9)
KAZ163	NLS1	19.4	0.22	0.16	9.8 (+1.3/-1.5)
MRK507	NLS1	9.74	0.23	0.23	23.3 (+1.0/-1.2)
MRK876	S1	169	0.1	0.04	–23 (+10/-23)
MRK885	S1.5	1.50	0.28	0.44	16.3 (+3.6/-2.1)
PGC61965	S1	727	0.13	0.08	0.90 (+0.33/-0.33)
UGC10697	S1	7.18	0.2	0.2	8.3 (+1.9/-1.8)

The Spitzer light curves for 11 of the 12 AGN are shown in Fig. 1. Only one object, Akn 524, exhibited no significant IR variability during the campaign. The most spectacular variations were seen in NGC6418, which underwent an outburst early in 2013 during which its 3.6 and 4.5 μm fluxes increased by factors ~2 in ~100 days (see Fig. 2 and panel below). Maximum variation amplitudes ΔF/<F> ~10% are more typical (see Table above), with timescales ranging from ~1 month to ~ 1 year. There is no clear correspondence with luminosity.

Cross-correlation analyses of the 4.5 and 3.6 μm light curve yields significant positive lags in 9/12 objects, ranging from ≈1 to 30 days (see Table and Figs 3 and 4). In addition, colour changes are seen in several cases, usually in the sense that the 4.5 μm flux exhibits stronger variability than the 3.6 μm flux (see Fig. 2, lower panel).

Vazquez 2015, Ph.D. Thesis, Rochester Institute of Technology (in prep.)

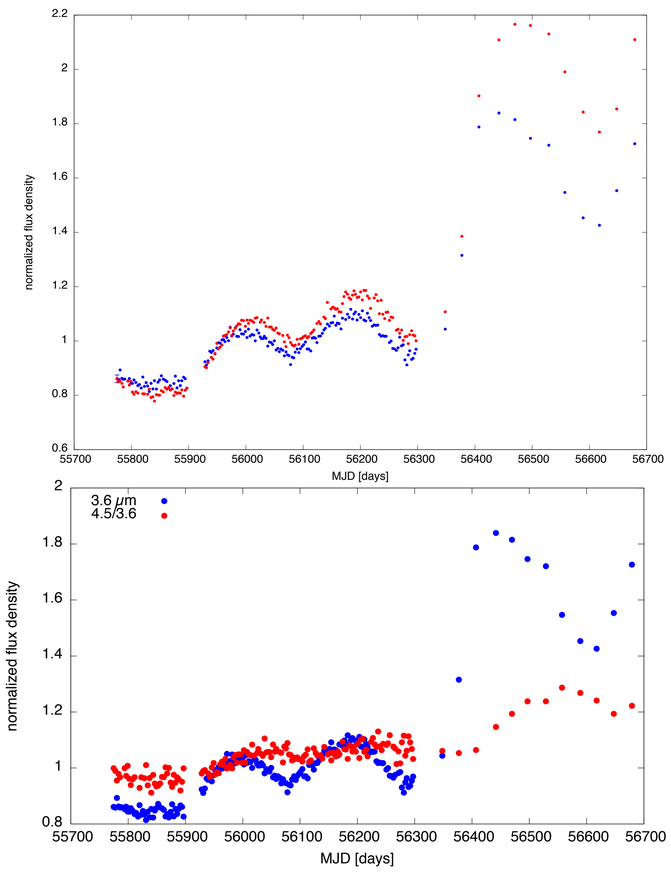

Fig. 2. Upper panel: as Fig. 1 for NGC6418. Lower panel: NGC6418 and several other objects (not shown) exhibit significant variations in the 4.5/3.6 flux ratio (red), which in this case, follows the 3.6 μm flux variations (blue) with a lag of ~50 days.

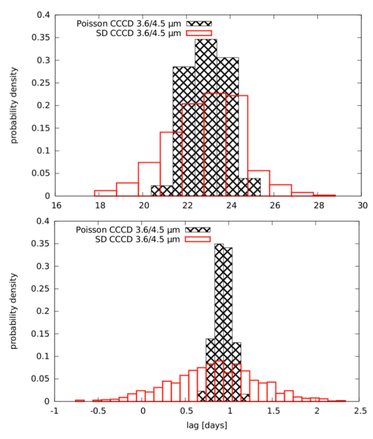

Fig. 3. Example cross-correlation centroid distributions (CCCD) for the 4.5 vs 3.6μm light curves. The CCCDs were constructed using a development of the the "Flux Randomization" technique of Peterson et al. (1998, PASP 110, 660). The lag values given in the table are derived from the histograms shown in red, for which the uncertainties on the flux measurements were derived from the light curve statistics rather than the standard poisson uncertainties on individual measurements.

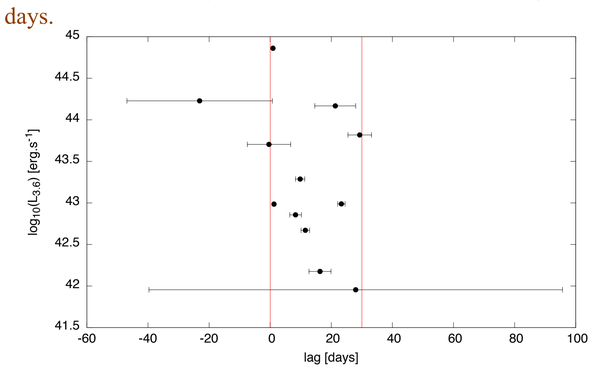

Fig. 4. Reverberation lag between 4.5 and 3.6 μm light curves. Variations in the 4.5 μm flux tend to lag behind those at 3.6 μm, by ~10 days. There appears to be no relation with luminosity.

Reverberation mapping NGC6418

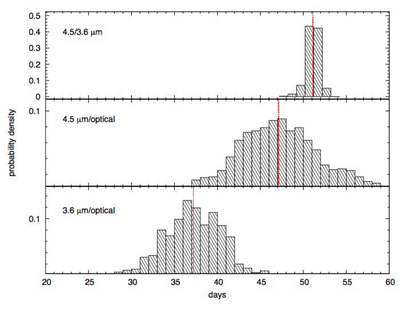

Fig. 5. Cross-correlation centroid distributions for Spitzer Cycle 8. The lag (indicated by the red line) is taken to be the median of the CCCD, with uncertainties given by the interquartile range. The 3.6 μm vs. 4.5 μm CCCD has been shifted by 37.2 days, the time lag between the 3.6 μm and optical light curves.

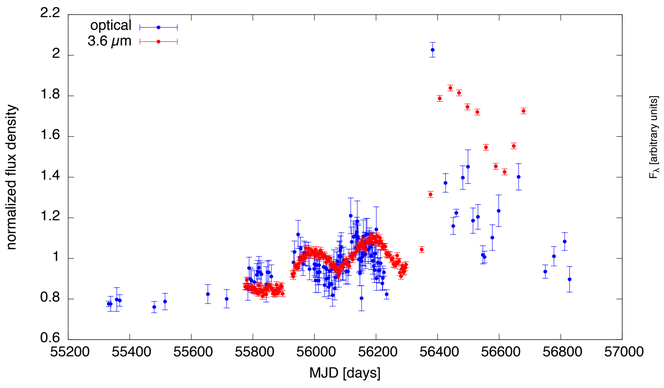

Fig. 6. Normalized optical (blue) and 3.6 μm (red) light curves for NGC6418. Unfortunately, the onset of the flare occurred when NGC6418 was unobservable from the ground. The peak is represented by only one measurement, but this is robust.

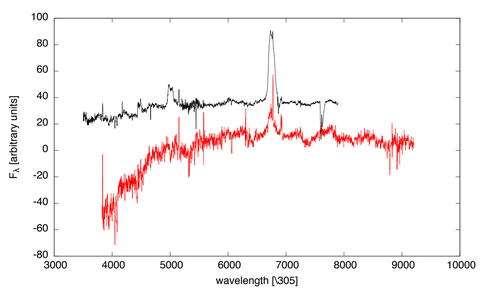

Fig. 7. Optical spectra of NGC6418 obtained by SDSS in Apr. 2001 (red) and by J. Gallimore at the APO 3.6 m in Jan. 2014 (black), approximately ~1 year after the outburst.

Cross-correlation analysis of the Cycle 8 optical and IR light curves (Fig. 5) shows that IR flux variations lag behind those of the optical continuum by ≈37±2 (3.6 μm) and ≈47±3 days (4.5 μm) indicating that the emitting dust is located at a distance ~1 light-month (~0.03 pc) from the AGN accretion disk. The lag between the 4.5 and 3.6 μm light curves is only ≈14 days, consistent with with clumpy torus models, in which individual optically thick clouds emit strongly over a broad wavelength range (see **Vazquez et al. 2015 ApJ, 801, 127**). Near the beginning of Cycle 9, a major outburst occurred during which the optical flux increased by a factor >2 in ≤100 days, before fading back to a level comparable with the mean Cycle 8 flux, while undergoing several lower amplitude variations (Fig. 6). A post-outburst optical spectrum exhibits much stronger broad lines and a much bluer continuum than are apparent in earlier observations (Fig. 7). The 3.6 μm and 4.5 μm fluxes responded with increased lags of 52 (+7,-4) and 74 (+2, -3) days, respectively. The lag between 4.5 μm and 3.6 μm fluxes increased to 20 ± 1 days (consistent with the difference between the 4.5 μm–optical and 3.6 μm–optical lags). The 4.5 μm/3.6 μm flux ratio also shows dramatic variations, which follow the 3.6 μm flux variations with a lag ~50 days (Fig. 2, lower panel). Evidently, this is because the 3.6 μm flux responds with a shorter delay but lower amplitude to the optical continuum.

R-L relation

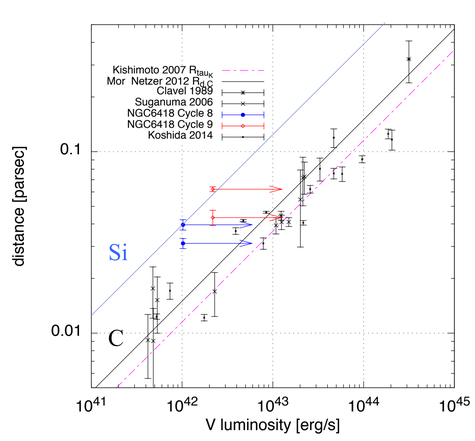

Fig. 8. Reverberation lag distance as a function of optical AGN luminosity. The plot shows K-band lags from Clavel et al. (1989, ApJ 337, 236), Suganuma et al. (2006, ApJ 639, 46) and Koshida et al. (2014, ApJ 788, 159), and the 3.6 and 4.5 μm lags for NGC 6418 (plotted as lower limits in luminosity as we only have a lower limit for the extinction). The dot-dashed line represents the $R \sim L^{0.5}$ fit to the K-band lags of Kishimoto et al. (2007, A&A 476, 713). The solid blue and black lines represent the sublimation radius for silicate and graphite dust grains, respectively.

The 3.6 and 4.5 μm reverberation radii fall above the $R \sim L^{0.5}$ relation found for previous K-band results (Fig. 8), as expected, but are similarly smaller (by a factor ~2) than the dust sublimation radius predicted for a typical ISM silicate grain mix. The increase in the lags following the optical outburst scales approximately with $L^{0.5}$.

RESEARCH POSTER PRESENTATION DESIGN © 2015
www.PosterPresentations.com